energies

MDPI

Article

Thermoeconomic Diagnosis of the Sequential Combustion Gas Turbine ABB/Alstom GT24

Sergio Castro-Hernández [1,*], Teresa López-Arenas [2], Edgar Vicente Torres-González [3], Helen Lugo-Méndez [2,*] and Raúl Lugo-Leyte [1]

[1] Departamento de Ingeniería de Procesos e Hidráulica, Universidad Autónoma Metropolitana—Iztapalapa, Av. San Rafael Atlixco No. 186, Col. Vicentina, Ciudad de México 09340, Mexico; lulr@xanum.uam.mx
[2] Departamento de Procesos y Tecnología, Universidad Autónoma Metropolitana—Cuajimalpa, Avenida Vasco de Quiroga No. 4871, Santa Fe, Cuajimalpa, Ciudad de México 05348, Mexico; mtlopez@cua.uam.mx
[3] Programa de Energía, Universidad Autónoma de la Ciudad de México, Plantel San Lorenzo Tezonco, Prol. San Isidro No. 151, Col. San Lorenzo Tezonco, Ciudad de México 09790, Mexico; edgar.vicente.torres.gonzalez@uacm.edu.mx
* Correspondence: sch@xanum.uam.mx (S.C.-H.); hlugo@cua.uam.mx (H.L.-M.)

Abstract: In this study, we used the thermoeconomic theory to evaluate the impact of residue cost formation on the cost of electricity generated from natural gas burned in a gas turbine that applied sequential combustion; we also analyzed the impact of the combustion process on the additional fuel consumption to compensate for a malfunction component. We used the Alstom GT24 gas turbine, which applied sequential combustion and generated 235 MW of power. Thermoeconomic analysis indicated that the exergy cost of power generation was 626.33 MW (30.42% corresponded to irreversibility costs, and 29.22% and 2.84% corresponded to the formation costs of physical and chemical residues, respectively). The exergoeconomic production cost of gas turbine was 10,098.71 USD/h, 34.76% from external resources and 65.24% from capital and operating costs. Thermoeconomic diagnosis revealed that a compressor deterioration (of 1-% drop in the isentropic efficiency) resulted in an additional fuel consumption of 4.05 MW to compensate for an increase in irreversibilities (1.97 MW) and residues (2.08 MW); the compressor generated the highest cost (49.9% of additional requirement). Thus, our study can identify the origin of anomalies in a gas-turbine system and explain their effects on the rest of the components.

Keywords: exergoeconomics; exergoeconomic costs; gas turbine; sequential combustion; residue; thermoeconomic theory; Alstom GT24 gas turbine; thermoeconomic diagnosis

check for updates

Citation: Castro-Hernández, S.; López-Arenas, T.; Torres-González, E.V.; Lugo-Méndez, H.; Lugo-Leyte, R. Thermoeconomic Diagnosis of the Sequential Combustion Gas Turbine ABB/Alstom GT24. *Energies* **2022**, *15*, 631. https://doi.org/10.3390/en15020631

Academic Editor: Tong Seop Kim

Received: 7 December 2021
Accepted: 12 January 2022
Published: 17 January 2022

Publisher's Note: MDPI stays neutral with regard to jurisdictional claims in published maps and institutional affiliations.

Copyright: © 2022 by the authors. Licensee MDPI, Basel, Switzerland. This article is an open access article distributed under the terms and conditions of the Creative Commons Attribution (CC BY) license (https://creativecommons.org/licenses/by/4.0/).

1. Introduction

Currently, the electricity power generation sector plays a key role in supplying the evergrowing worldwide energy demand, at the expense of an increase in the consumption of fossil resources and a negative environmental impact. In the past, energy, exergetic, economic, and optimization analyses have been developed and implemented to encourage sustainability and mitigate the adverse effects of this sector [1–3]. Exergetic analyses have identified the causes of irreversibilities and inefficiencies in an energy system [4], which are inversely related: low irreversibility leads to high exergetic efficiencies and, therefore, low energy production costs.

Thermoeconomic theory, also known as exergoeconomics, is used to evaluate both the exergetic and economic performances of productive systems. This discipline is based on exergy and the productive purpose of energy systems, and its objective is to systematically account the costs of material and energy streams [5–7]. A disadvantage of the application of thermoeconomic analysis is the ambiguous definition of the useful product(s) of a system. Such ambiguity can be overcome using experienced analysts and by understanding

the scope of the study [7–9]. This systematic cost accounting methodology is based on algebraic equations and focuses on the rational allocation of the production and residue cost formation processes of a system [10,11].

Most thermoeconomic cost accounting methodologies only consider the production process of the system, while overlooking both the product and residue cost formation processes. A residue is an exergy loss; its formation cost must be charged to the production cost of the system, as well as the cost of internal streams. For this reason, it is necessary to impute the participation of the productive components of a system in the formation of residues, to properly determine the costs of the useful product and residues. Notably, previous studies have explained a costing process for functional products like a costing process for residues [12–14].

There is no single methodology to allocate the cost formation process of residue to the productive components of a system [15,16]. Some allocation criteria reported in the literature include the distribution cost of residues proportional to entropy generation (or negentropy) [5,17], exergy [8], distributed entropy [18], and irreversibility [19].

Valero et al. [13,20] developed thermoeconomic methodologies that include the formation processes of both the functional product and the residue in the accounting of the costs of internal flows in a system, along with the costs of the product and residue, and applied the distributed exergy criterion to attribute the cost of the residue to the productive components. This contribution has been used to study the production and formation costs of residues from energy systems, with respect to combined cycles [14,18], heating and cooling systems [8], and aviation [19], among others. Likewise, Valero et al. proposed an exergoeconomic methodology known as symbolic thermoeconomics, in which a productive scheme was developed from the physical structure of the study system, also known as the productive structure, while analyzing the distribution of exergy flows throughout the system and the interaction of the system with the environment [12,21]. This methodology formulates two alternative representations for the productive structure of a system: fuel-product-residue (FPR) and product-fuel-residue (PFR). The FPR representation is mainly adopted for cost accounting, while the PFR representation is used more for thermoeconomic diagnosis [19]. The thermoeconomic diagnosis compares two operating conditions (actual and design) to quantify, with respect to additional consumption of resources, the effect generated by the malfunction of a component within a system that aims to generate the same useful product [22–25].

Motivated by the above-mentioned research, our study presents an exergoeconomic diagnosis, based on symbolic thermoeconomics, of a gas turbine with sequential combustion considering the formation processes of both functional product and residues. Since gas turbine systems are the core components in electric power generation plants, determining their electricity generation costs and the formation cost of residues is of vital importance. Gas turbine systems with sequential combustion generate extra power by burning an extra amount of fuel with the combustion gases produced in the combustion chamber of the gas turbine. This means that sequential combustion gas turbines take advantage of the combustion gases exergy to produce electric power, and their environmental impact has been discussed in [26,27].

This manuscript is organized into six sections. In Section 2, a brief description of the study system is presented, which corresponds to an Alstom GT24 gas turbine that operates under a post-combustion process and produces a power of 235 MW under specific design conditions. In Section 3, the energetic and exergetic models of the system are described to estimate their thermodynamic states. In the same section, the productive structure of the system is established, along with explaining the resource, product, and residue of the components that make up the gas turbine. Section 4 summarizes the mathematical basis for cost evaluation and the residue formation process. Section 5 deals with the thermoeconomic diagnosis of the system and discusses the different impacts of different decompositions on the fuel used in the system: irreversibilities and residues, unit exergy costs of resources and residues, and malfunctions and dysfunctions. The thermoeconomic diagnosis was

carried out to quantify the effects of the deterioration of the compressor (malfunction) on the rest of the gas turbine components. Finally, the main contributions of this study and discussions on the results are summarized in Section 6.

2. Case Study

The case study considers the ABB/Alstom GT24 reheat gas turbine, shown in Figure 1, operating under a sequential combustion cycle. In the turbine, the air enters the 22-stage centrifugal compressor (C) under ambient conditions (g1). The compressed air (g2) leaving the compressor is mixed with natural gas in the annular combustion chamber (CC1), and their reaction produces combustion gases (g3). These gases are then, expanded in a single-stage high-pressure turbine (HPT) to generate work. These combustion gases are fed to a second annular combustion chamber (CC2) to react with additional fuel (g5) and reach the same temperature as that in the first reaction. Finally, in a four-stage low pressure turbine (LPT), the combustion gases expand to atmospheric pressure (g6). to generate work.

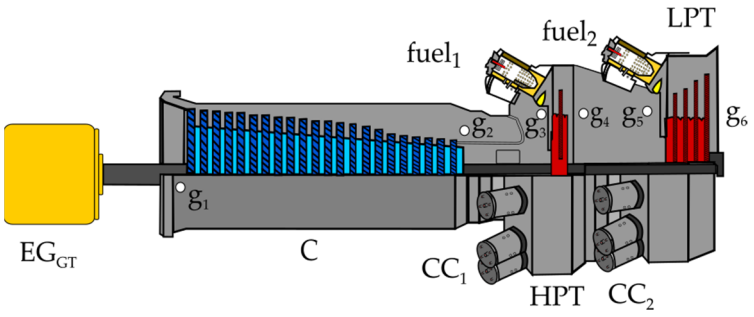


Figure 1. Schematic diagram of ABB/Alstom GT24 equipped with afterburner; electric generator (EG_{GT}), air at ambient conditions (*a*), centrifugal compressor (C), air (g_1), first annular combustion chamber (CC_1), combustion gases (g_3), high-pressure turbine (HPT), combustion gases (g_4), second annular combustion chamber (CC_2), additional fuel (g_5), low pressure turbine (LPT), and combustion gases expanded to atmospheric pressure (g_6).

Study Considerations

- The system operates at a steady state.
- The working fluids are considered perfect gases.
- The temperature and pressure of the dead state were T_0 = 10 °C and P_0 = 0.80 bar.
- The molar composition of natural gas was: 0.9687 CH_4; 0.0285 C_2H_6; 0.0024 C_3H_8; 0.0003 *n*-C_4H_{10}; and 0.0001 *i*-C_4H_{10} [11].
- The low heating value (*LHV*) of natural gas was 49,854.53 kJ/kg_{fuel}.

3. Energy and Exergy Analysis

Table 1 presents the expressions of the temperature (*T*) and pressure (*P*) of each thermodynamic state of the gas turbine, in terms of the technological parameters such as the efficiency (η), pressure ratio (π), turbine inlet temperature (*TIT*) and ratio of the particular gas constant to heat capacity of constant pressure (x) of the air (*a*) and combustion gases (cg). This table is obtained from the energy analysis of the system.

The air mass flow rate ($\dot{m}_a$) entering the gas turbine obtained from the power of the gas turbine ($\dot{W}_{GT}$) and motor work (w_m) can be explained using the following equation:

$$\dot{m} = \frac{\dot{W}_{GT}}{w_m} \tag{1}$$

where

$$w_m = (far_2 + far_1 + 1)w_{HPT} + (far_1 + 1)w_{LPT} - w_C \tag{2}$$

w_{HPT}, w_{LPT}andw_C represent the motor work of the high and low pressure turbines and the compressor, respectively. The fuel-to-air ratios (*far*) of the combustion reactions in combustion chambers 1 and 2 were obtained from the mass and energy balances in the corresponding combustion chambers, which can be expressed as follows:

$$far_1 = \frac{h_3 - h_2}{LHV - h_3} \tag{3}$$

$$far_2 = \frac{(far_1 + 1)(h_5 - h_4)}{LHV - h_5} \tag{4}$$

Table 1. Thermodynamic properties of the GT cycle.

State		Temperature	Pressure
g_1	$\dot{m}_a$	T_a	P_a
g_2	$\dot{m}_a$	$T_2 = T_1\left[1 + \frac{1}{\eta_C}\left(\pi_C^{x_a} - 1\right)\right]$	$P_1\pi_C$
g_3	$\dot{m}_{cg1}$	TIT	$P_3 = P_2\left(1 - \frac{\Delta P_{CC_1}}{P_2}\right)$
g_4	$\dot{m}_{cg1}$	$T_4 = T_3\left[1 - \eta_T\left(1 - \frac{1}{\pi_{TAP}^{\frac{x_{cg}}{}}}\right)\right]$	$P_4 = P_5\left(1 + \frac{\Delta P_{CC_2}}{P_5}\right)$
g_5	$\dot{m}_{cg2}$	TIT	$P_5 = \frac{P_6}{\left[1 - \frac{1}{\eta_T}\left(1 - \frac{T_6}{T_5}\right)\right]^{\frac{1}{x_{cg}}}}$
g_6	$\dot{m}_{cg2}$	T_{eg}	P_a

Therefore, the fuel flows are obtained from

$$\dot{m}_{fuel_1} = \dot{m}_a far_1 \; and \; \dot{m}_{fuel_2} = \dot{m}_a far_2 \tag{5}$$

The enthalpy $\left(\dot{H}\right)$, entropy $\left(\dot{S}\right)$, and physical exergy $\left(\dot{E}^{PH}\right)$ flows for the thermodynamic states were estimated using the following expressions:

$$\dot{H}_i = \dot{m}_i c_{Pi}\left(T_i - T_{ref}\right) \tag{6}$$

$$\dot{S}_i = \dot{m}_i\left[s_{ref} + c_{pi}\ln\left(\frac{T_i}{T_{ref}}\right) - R_i\ln\left(\frac{P_i}{P_{ref}}\right)\right] \tag{7}$$

$$\dot{E}_i^{PH} = \dot{H}_i - \dot{H}_0 - T_0\left(\dot{S}_i - \dot{S}_0\right) \tag{8}$$

The chemical exergy flow ($\dot{E}^{CH}$) of an ideal gas mixture, in terms of the molar mass (*MW*), standard molar chemical exergy (ε_{0j}) and molar composition (x_j) of the species in the mixture [8], can be expressed as follows:

$$\dot{E}_i^{CH} = \frac{\dot{m}_i}{MW_i}\sum_{j=1}^{N_c}\left(x_j\varepsilon_{0j} + T_0\, R_u\, x_j\, \ln\, x_j\right) \tag{9}$$

For i = 1, 2 the working fluid was air, while for i = 3, 4, and i = 5, 6, the working fluids corresponded to the combustion gases produced in both the combustion chambers. In CC_1, the combustion of natural gas ($C_{1.034}H_{4.069}$; n = 1.034, m = 4.069) with excess air (λ) occurred according to the following chemical reaction:

$$C_nH_m + \left(n + \tfrac{m}{4}\right)(1 + \lambda)(O_2 + 3.76N_2) \rightarrow$$
$$nCO_2 + \tfrac{m}{2}H_2O + 3.76\left(n + \tfrac{m}{4}\right)(1 + \lambda)N_2 + \left(n + \tfrac{m}{4}\right)\lambda\, O_2$$

An additional amount of natural gas ($\dot{m}_{fuel2}$) was post-combusted in CC_2, using the oxygen from the combustion gases produced in CC_1. The afterburner chemical reaction can be expressed as follows:

$$C_nH_m + nCO_2 + \frac{m}{2}H_2O + 3.76\left(n + \frac{m}{4}\right)(1+\lambda)N_2 + \left(n + \frac{m}{4}\right)\lambda O_2 \rightarrow$$
$$2nCO_2 + mH_2O + 3.76\left(n + \frac{m}{4}\right)(1+\lambda)N_2 + \left(n + \frac{m}{4}\right)(\lambda - 1)O_2$$

Table 2 presents the design technological parameters of the gas turbine used to determine the thermodynamic properties listed in Table 1.

Table 2. Technological parameters of the ABB/Alstom GT24 system uses in our study.

$\dot{W}$, (kW)	235,000	η_C (-)	0.88
TIT, (°C)	1250	η_T, (-)	0.9
T_6, (°C)	616	ΔP_{CC}, (bar)	0.04
π_C, (-)	30	LHV, (kJ/kg$_{fuel}$)	49,854.532

From the combustion reactions and the energy balances in the combustion chambers of the GT24 operating under the conditions listed in Table 2, it is determined that 1) the excess air required to reach the combustion temperature of the gases leaving the first combustion chamber (1250 °C) is 211.96%; and 2) the compositions of the combustion gases produced in both combustion chambers, which are used to calculate the heat capacity c_P and $x = R/c_P$ shown in Table 3.

Table 3. Thermodynamic properties of combustion gases.

	c_{Pcg} (kJ/kgK)	c_{Vcg} (kJ/kgK)	R_{cg} (kJ/kgK)	g_{cg} (-)	$x_{cg} = R_{cg}/c_{Pcg}$ (-)
CC_1	1.3255	1.0331	0.2924	1.28	0.2206
CC_2	1.4189	1.1225	0.2964	1.26	0.2089

The gas turbine GT24 generated a net power of 235 MW by burning 10.16 kg$_{fuel}$/s of natural gas in CC_1, with an air flow rate of 440.16 kg$_a$/s, along with an additional fuel supply of 2.40 kg$_{fuel}$/s in the CC_2. The thermodynamic states of the GT24 cycle operating under the conditions listed in Table 2 are provided in Table 4. The thermodynamic states g_3 and g_5 indicated the highest physical exergy flows of the process because they had the highest pressures and temperatures in the cycle, owing to the compression and combustion processes (Figures 2 and 3). The material streams of combustion gases associated with states g_5 and g_6 presented the highest chemical exergy flowrates produced during the combustion of natural gas. These exergy streams were not used to generate the power of the system, and thus, they were waste streams. The GT24 afterburner gas turbine had a thermal efficiency of 32.14% and an exergy efficiency of 37.52%.

Table 4. Thermodynamic states of the sequential gas turbine cycle applied in our study.

State	$\dot{m}_a$ (kg/s)	T (K)	P (bar)	$\dot{H}$ (MW)	$\dot{S}$ (MW/K)	$\dot{E}^{PH}$ (MW)	$\dot{E}^{CH}$ (MW)
g_0	-	283.15	0.80	-	-	-	-
g_1	440.16	283.15	0.80	0	2.91	0	1.95
g_2	440.16	811.68	24.09	235.85	2.94	224.98	1.95
g_3	450.32	1523.15	23.61	742.40	3.54	583.30	7.70
g_4	450.32	1420.54	16.58	680.96	3.54	520.49	7.70
g_5	452.72	1523.15	16.25	800.74	3.67	607.49	19.75
g_6	452.72	889.15	0.82	391.33	3.73	182.99	19.75

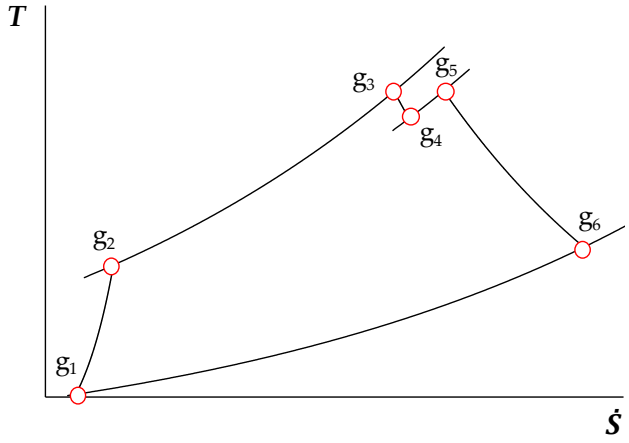


Figure 2. Temperature-entropy ($\dot{T}$-$\dot{S}$) graph of the sequential gas turbine (GT) cycle.

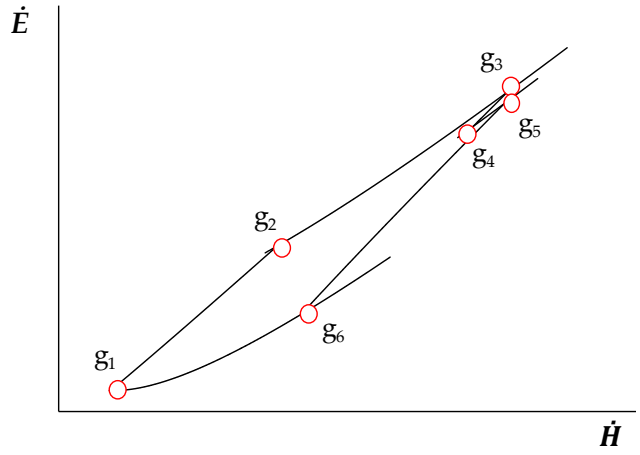


Figure 3. Exergy-enthalpy flow ($\dot{E}$-$\dot{H}$) of the sequential gas turbine (GT) cycle.

Each productive component of the GT24 used a resource ($\dot{F}$) to produce $\dot{P}$ units of exergy and destroyed a part of the fueled exergy accounted in the internal irreversibility, $\dot{I} = \dot{F} - \dot{P}$. These exergy flows were established according to the productive purpose of the components, and their computed values are listed in Table 5. The compressor resource is the compression power, and its product is the increment of air physical exergy; the two combustion chambers are fueled with their respective natural gas exergy flows to produce the chemical exergy of combustion gases and increase the physical exergy of the mixture (of excess air and combustion gases) by heating it up to the required temperature at the turbine inlet. The resources of the LPT and HPT is the difference in the combustion gas exergy at the entrance and exit, and their product is their generated power.

Table 5. Resource, product, and internal irreversibility of ABB/Alstom GT24 components.

Component	$\dot{F}$ (MW)	$\dot{P}$ (MW)	$\dot{I}$ (MW)	$\dot{R}$ (MW)	η_{ex} (-)
C	235.85	224.98	10.86	61.42	0.95
CC_1	506.55	364.06	142.49	103.57	0.72
HPT	62.80	61.43	1.37	0	0.98
CC_2	119.78	99.05	20.73	35.80	0.83
LPT	424.50	409.41	15.09	0	0.96
GT24	626.33	235.00	190.54	200.79	0.375

Note: Compressor (C), first annular combustion chamber (CC_1), high-pressure turbine (HPT), second annular combustion chamber (CC_2), low-pressure turbine (LPT), gas turbine (GT).

A graphical representation of the exergy distribution flows reported in Table 5 is shown in the Grassmann diagram of GT24 depicted in Figure 4. The external resource of the gas turbine was the chemical exergy of the natural gas fed to the combustion chambers CC_1 and CC_2, corresponding to $\dot{F}_1$ = 506.55 MW and $\dot{F}_2$ = 119.78 MW, respectively. The exergy efficiency of the gas turbine indicated that 37.52 % of the fuel exergy supplied to GT24 was used to generate 235 MW of useful power, 30.06 % was delivered to the environment through the physical ($\dot{R}^{PH}$ = 182.99 MW) and chemical ($\dot{R}^{CH}$ = 17.80 MW) exergy of the exhausted gases, and the rest of the exergy was internally destroyed in the components of the system.

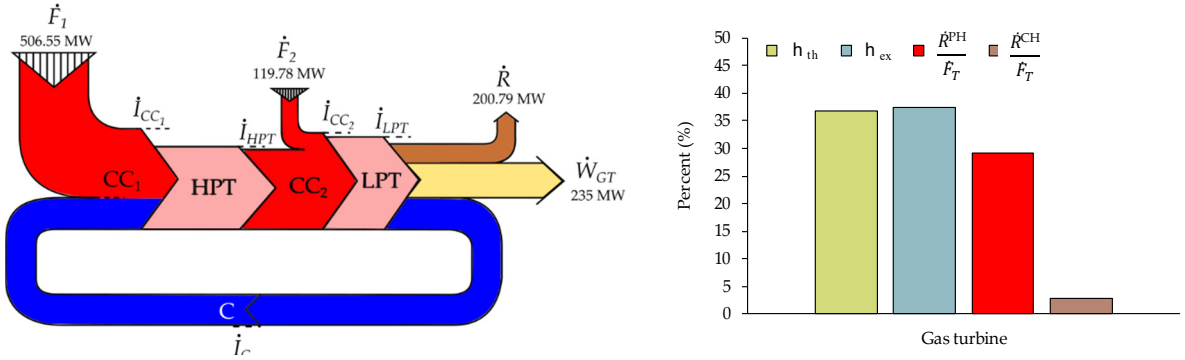


Figure 4. Grassmann Diagram of the ABB/Alstom GT24 system.

4. Thermoeconomic Analysis

A productive structure is a graphic representation of the distribution of internal resources and products in an energy system using a physical model as a reference [13]. The products of each productive component serve as resources for other components to form the main products, by-products, and residues [19]. The productive components are those that provide resources to other components to form the final products and residual streams of an energy system.

The productive structure of the ABB/Alstom gas turbine GT24 is shown in Figure 5; the external resource was the fuel exergy flow ($\dot{E}_{fuel}$) entering the two combustion chambers (CC_1 and CC_2) used to generate the useful power and form the residual combustion gas streams of physical and chemical exergy. The functional products of the compressor and combustion chambers contributed to increasing the physical exergy of the combustion gases, which served the HPT and LPT to produce their respective powers. A fraction of the power generated by the expansion turbines was supplied to the compressor to increase the physical exergy of the air.

The productive structure indicated that the formation process of gas turbine power, EW_{GT}, was parallel to the formation of physical ($\dot{R}^{PH} = \dot{E}g_6{}^{PH}$) and chemical ($\dot{R}^{CH} = \dot{E}_T{}^{CH}$) residues. Figure 5 also indicates that the compressor and combustion chambers are the productive components to which the formation of physical exergy flow of the combustion gases is allocated to and that the combustion chambers are the unique components charged to form the chemical exergy of combustion gases. The physical exergy is processed within the productive components to be supplied as a resource of another component or to become a residual stream. This study analyzes the cost formation process of GT24 (based on the productive structure provided in Figure 5) and the development of the FPR thermoeconomic model.

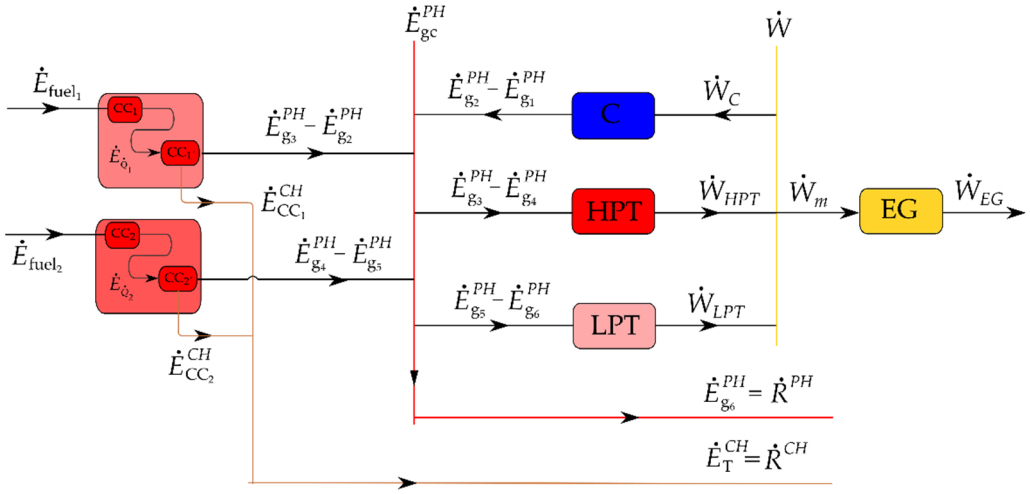


Figure 5. Productive structure of the ABB/Alstom sequential-combustion gas turbine GT24.

The FPR model quantifies the amount of exergy supplied to the system that is used as a resource in the productive components to form the functional product, it allows the computation of the fraction of the product of such components serving as a resource for the other components. To analyze the formation process of the residues of the gas turbine, the FPR model determines the allocation relations between the exergy of residues and the products of the components participating in its production by defining the distribution coefficients (y_{ij}, ψ_{ij}). These ratios quantify the amount of product by the j-th component (used as a resource) or the residue by the i-th component, which can be expressed as follows:

$$\left\{ y_{ij} = \frac{\dot{E}_{ji}}{\dot{P}_j} \right\}_{nxn} = \langle \mathbf{FP} \rangle, \ \sum_{i=0}^{n} y_{ij} = 1 \tag{10}$$

$$\left\{ \psi_{ij} = \frac{\dot{R}_{ji}}{\dot{P}_j} \right\}_{nxn} = \langle \mathbf{RP} \rangle, \ \sum_{i=0}^{n} \psi_{ij} = 1 \tag{11}$$

where $\dot{E}_{ij}$ is the product of the i-th productive component used as a resource by the j-th component, and $\dot{R}_{ij}$ is the exergy of the residue i-th imputed to the j-th component.

The distribution coefficients obtained from the FPR model for the sequential gas turbine are listed in Table 6. The $\langle \mathbf{FP} \rangle$ matrix indicates how the product of the productive components C, CC_1, and CC_2 were used as resources by the high and low-pressure turbines (HPT and LPT) in proportions of 0.34, 0.53, and 0.13, respectively. The products of the turbines served as resources only for the compressor (C) and the electric generator (EG) in fractions of 0.13 and 0.87, respectively. The $\langle \mathbf{RP} \rangle$ matrix contained the contributions of the products of the components participating in the formation of residues. In this way, the physical exergy of the exhaust gases ($\dot{R}^{PH} = \dot{E}_{g6}$) was estimated from the products of the compressor (at a ratio of 0.34) and the CC_1 and CC_2 in fractions of 0.53 and 0.13, respectively. Whereas, the residue associated with the chemical exergy of the combustion gases, $\dot{R}^{CH} = \dot{R}^{CH}_{CC1} + \dot{R}^{CH}_{CC2}$, only formed by the combustion processes in CC_1 and CC_2 in proportions of 0.32 and 0.38, respectively.

Table 6. Fuel-product-residue (FPR) Model of the ABB/Alstom gas turbine GT24.

				<FP>				<RP>	
	$\dot{F}_0$	$\dot{F}_C$	$\dot{F}_{CC1}$	$\dot{F}_{HPT}$	$\dot{F}_{CC2}$	$\dot{F}_{LPT}$	$\dot{F}_{EG}$	$\dot{R}^{PH}$	$\dot{R}^{CH}$
$\dot{P}_0$			1.00		1.00				
$\dot{P}_C$				0.34		0.34		0.34	
$\dot{P}_{CC1}$				0.53		0.53		0.53	0.32
$\dot{P}_{HPT}$		0.13					0.13		
$\dot{P}_{CC2}$				0.13		0.13		0.13	0.68
$\dot{P}_{LPT}$		0.87					0.87		
$\dot{P}_{EG1}$	1.00								
Total	1.00	1.00	1.00	1.00	1.00	1.00	1.00	1.00	1.00

4.1. Residue Formation Costs

Thermoeconomics is based on the premise that residues are formed within the productive components and that they are released into the environment through dissipative components. The productive components are those that provide resources to other components to form the final products and residual streams of an energy system [14]. In dissipative components, the exergy of the residue is totally or partially destroyed using additional external resources, whose costs are known as disposal or abatement costs and are charged to the productive components of the system [13].

The exergoeconomic cost of a residue disposed into the environment by a dissipative component is conformed by its formation cost, which is the cost of the exergy flow serving as a resource to the dissipative component (Π_{f_r}) (formed in the productive components system), cost of additional exergy resources used for its elimination (Π_{a_r}), and the maintenance and operation non-exergy costs (Z_r) [3,20], which can be expressed as follows:

$$\Pi_{P_r} = \Pi_{f_r} + \Pi_{a_r} + Z_r \tag{12}$$

In this study, we assumed that the residue was discharged into the environment by means of imaginary dissipative components, denoted as physical and chemical stacks (PHS and CHS, respectively). For the gas turbine system, the cost of the total residue $(\Pi_{P_{Tr}})$ was the sum of the costs of each residue, which can be expressed as follows:

$$\Pi_{P_{Tr}} = \Pi_{P_r}^{PH} + \Pi_{P_r}^{CH} \tag{13}$$

The allocation of the cost of the residue released into the environment from the dissipative unit r and formed in component i $\left(\Pi_{P_{ri}}\right)$ can be expressed as follows:

$$\Pi_{P_{ri}} = \psi_{ir}\Pi_{P_r}^{k},\ k = \text{PH, CH} \tag{14}$$

where ψ_{ir} is the allocation coefficient of the i-th productive component participating in the formation of the r-th residue. These coefficients were determined from the application of one of the residue cost allocation criteria reported in the literature [13,17]. In this study, we employed the distributed exergy criterion formulated by Valero et al. [13], in which ψ_{ir} is the relationship between the exergy of the residue formed in the i-th productive component and the exergy fed to the r-th dissipative component (distribution coefficients, see Equation (14)) [12], according to the productive structure of the system, obtained directly from the FPR (Table 6).

4.2. Process for Allocating Costs to Products and Residue

The production cost of the *i*-th component (Π_{Pi}) is integrated by the cost of the product of the *i*-th component that served as resource for the *j*-th component ($\Pi_{P_{ij}}$) and to the *r*-th dissipative component ($\Pi_{P_{ir}}$)

$$\Pi_{P_i} = \Pi_{P_{ij}} + \Pi_{P_{ir}} \tag{15}$$

The balance of exergoeconomic costs of the extended productive component with the dissipative component were calculated using the following equation:

$$\Pi_{P_{ij}} = \Pi_{F_i} + Z_i + Z_r + \Pi_{a_r} \tag{16}$$

Substituting Equations (12) and (16) in (15), it turns out that

$$\Pi_{P_i} = \Pi_{F_i} + \Pi_{P_r} + Z_i \tag{17}$$

In matrix notation [13], this can be expressed as follows:

$$\mathbf{\Pi}_P = \mathbf{\Pi}_F + \mathbf{\Pi}_R + \mathbf{Z} \tag{18}$$

where

$$\mathbf{\Pi}_P = (\mathbf{U}_D - \langle \mathbf{FP} \rangle - \langle \mathbf{RP} \rangle)^{-1} (\mathbf{\Pi}_e + \mathbf{Z}) \tag{19}$$

$$\mathbf{\Pi}_F = \mathbf{\Pi}_e + \langle \mathbf{FP} \rangle \mathbf{\Pi}_P \tag{20}$$

$$\mathbf{\Pi}_R = \langle \mathbf{RP} \rangle \mathbf{\Pi}_P \tag{21}$$

The exergy theory states that the balance of the exergoeconomic costs of the productive component is the sum of their resource exergoeconomic costs of the system, and the exergy costs are obtained in the same way, but as exergy flow units, without considering the operation, maintenance, and amortization costs (**Z**). This can be expressed as follows:

$$\mathbf{P}^* = \mathbf{F}^* + \mathbf{R}^* \tag{22}$$

Table 7 presents the exergy cost of the resource, product, and residue of each of the components that constitute the gas turbine cycle. This table indicates that the exergy costs of the product and resource were the same for the HPT, LPT, and EG, because these components did not participate in the formation of any residue in the system. However, because the compressor and combustion chambers were involved in the formation of the residue, then, according to Equation (22), the exergy costs of the product were higher than those of the resource. The exergy cost of generating electricity from the regenerative gas turbine was 626.33 MW, while the cost of residue formation was 505.24 MW, which represented 80.67% of the total exergy cost of electricity.

Table 7. Exergy costs of the resource and product of the equipment of ABB/Alstom GT24 system.

	P* **(MW)**	**F*** **(MW)**	**R*** **(MW)**
C	864.63	628.58	236.04
CC_1	707.95	506.55	201.40
HPT	161.73	161.73	0.00
CC_2	187.59	119.78	67.81
LPT	1093.19	1093.19	0
GT	626.33	626.33	0

The exergy cost of a stream, $E_i^* = \dot{E}_i + \sum_{pro}(\dot{I} + \dot{R})$, is the sum of its exergy and the internal and external irreversibility of the productive components accumulated throughout the production process. The production structure presented in Figure 5 indicates that the electric power generation process in the gas turbine system began in CC_1 and CC_2.

Therefore, with respect to CC_1 and CC_2, the exergetic costs of these components were affected only by their own irreversibilities (199.14 MW and 32.48 MW, respectively) and by the formation of physical (136.71 MW and 37.20 MW, respectively) and chemical (8.03 MW and 18.88 MW, respectively) residue, as shown in Figure 6. The remaining productive components used a portion of their products as resource, and the exergy cost of their products involved the internal and external irreversibilities accumulated in the previous processes. The exergy cost of generating electricity from the gas turbine system was 626.33 MW, of which, the exergy flow, irreversibilities, physical residue flows, and chemical residue flows were 235, 190.54, 182.99, and 17.80, respectively.

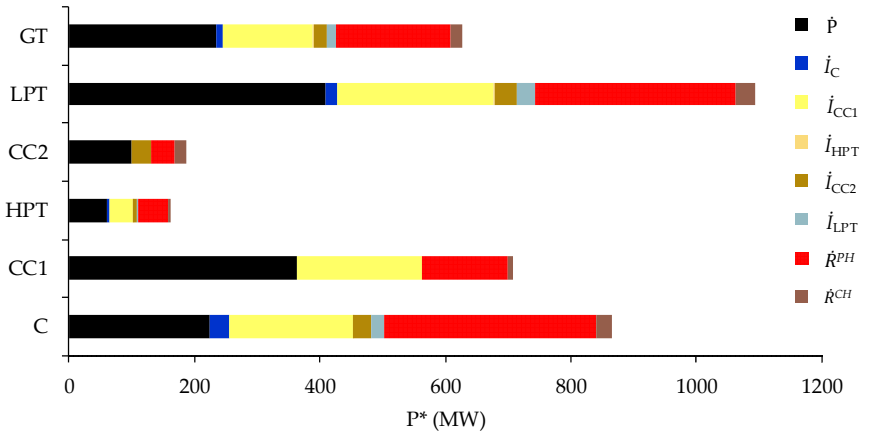


Figure 6. Exergy cost of the products of the gas turbine components with respect to regeneration; Compressor (C), first annular combustion chamber (CC_1), second annular combustion chamber (CC_2), high-pressure turbine (HPT), low-pressure turbine (LPT), gas turbine (GT).

The exergoeconomic costs associated with the product, resources, and residue are presented in Table 8. According to Equation (19), the exergoeconomic cost of the product of each component of the system is made up of the cost of external resources (Π_e) used, along with the cost of operation, maintenance, and amortization of the equipment. In this study, CC_1 and CC_2 were the only components whose exergoeconomic cost of production depended on the cost of external resources, because they were supplied with fuel at a cost of 5328.34 USD/h and 1259.96 USD/h, respectively.

Table 8. Exergoeconomic costs for different components of the ABB/Alstom GT24 system used in our study.

	Π_e (USD/h)	Π_P (USD/h)	Π_F (USD/h)	Π_R^{PH} (USD/h)	Π_R^{CH} (USD/h)	Z (USD/h)
C	0	16,883.18	10,135.06	4609.10	0	2139.02
CC_1	5328.34	7542.28	5328.34	2026.52	119.10	68.32
HPT	0	2578.70	2448.72	0	0	129.97
CC_2	1259.96	2083.06	1259.96	499.48	253.47	70.15
LPT	0	17,655.07	16,552.13	0	0	1102.95
TG		10,098.71	10,098.71	7507.67		3510.41

Equation (21) established that the cost of the residue is the sum of the product of the production costs of the productive components and the distribution coefficients of the residue. In our study, the cost of formation of the physical residue was 7135.10 USD/h, to which the compressor, CC_1, and CC_2 contributed 4609.10 USD/h, 2026.52 USD/h, and 499.48 USD/h, respectively. The chemical residues generated in CC_1 and CC_2 had costs of 119.10 USD/h and 253.47 USD/h, respectively.

Finally, the cost of generating electricity was 10,098.71 USD/h, of which 3510.41 USD/h corresponded to the cost of the equipment and 6588.30 USD/h corresponded to the external resources that entered the system.

5. Thermoeconomic Diagnosis

Our diagnosis was based on identifying and understanding the malfunction of any system and quantifying its effects on the components of the system, environment, demand for resources, generation of products, and residue [22]. With respect to the thermoeconomics of the system, the malfunction was quantified through the additional consumption of resources necessary to obtain the same exergetic flow of the product in a current operating condition of the system ($\mathbf{x}$), with respect to a reference ($\mathbf{x}_0$), $\Delta\dot{F}_T = \dot{F}(\mathbf{x}) - \dot{F}(\mathbf{x}_0)$.

In this study, a thermoeconomic diagnosis of a gas turbine that generated 235 MW was carried out, considering that the compressor presented an anomaly corresponding to the decrease in its isentropic efficiency by 1%. Table 9 shows the exergy flows, which serve as a resource, product, irreversibility, and residue, for each productive component of the system under design conditions ($\mathbf{x}_0$) and current operation ($\mathbf{x}$). The table indicates that, for the gas turbine to generate the same power, an additional 4.05 MW of fuel is required to be fed into CC_1 and CC_2 to compensate for compressor malfunction.

Table 9. Exergy flows of gas turbine components under current design and operating conditions.

	Design				**Actual**			
	$\dot{F}$	$\dot{P}$	$\dot{I}$	$\dot{R}$	$\dot{F}$	$\dot{P}$	$\dot{I}$	$\dot{R}$
	MW				**MW**			
C	235.85	224.98	10.86	0	240.72	228.91	11.82	0
CC_1	506.55	364.06	142.49	0	509.36	366.24	143.12	0
HPT	62.80	61.43	1.37	0	63.45	62.07	1.38	0
CC_2	119.78	99.05	20.73	0	121.02	100.08	20.94	0
LPT	424.50	409.41	15.09	0	428.90	413.65	15.25	0
GT	626.33	235.00	190.54	200.79	630.38	235.00	192.51	202.87

The additional consumption of resources fed to the system, $\Delta\dot{F}_T$ = 4.05 MW, was the exergy that the system could save by operating even with the compressor malfunction. This impact on fuel consumption corresponded to 1.03% of the total irreversibilities (internal and external) of the system operating with the anomaly (395.38 MW). The exergy analysis revealed that the deterioration of the compressor required additional fuel consumption, which resulted in adjustments of the consumption and production of exergy in each component, along with the irreversibility and contribution of the components to the formation of residue. This thermoeconomic diagnosis based on exergetic analysis is known as technical savings and consists of decomposing the additional consumption of resources as the sum of the variation of irreversibilities and residuals, $\Delta\dot{F}_T = \Delta\dot{I}_T + \Delta\dot{R}_T$. However, it does not allow the identification of the real causes of the anomaly.

5.1. Fuel impact

The total external resource fed to the system expressed in terms of the unit consumption of the resources that enter the system (${}^t\boldsymbol{\kappa}_e = \kappa_{01}, \ldots, \kappa_{0n}$) and the product of each component can be expressed as: $\dot{F}_T = {}^t\boldsymbol{\kappa}_e\mathbf{P}$. Based on this expression, Valero et al. [19] obtained the impact on fuel (additional resource consumption, $D\dot{F}_T$) of a system operating in a current condition ($\mathbf{x}$) with respect to a design one ($\mathbf{x}_0$), which can be expressed as $D\dot{F}_T = D^t\boldsymbol{\kappa}_e\mathbf{P}(\mathbf{x}_0) + {}^t\boldsymbol{\kappa}_e D\mathbf{P}(\mathbf{x}_0)$. This relationship can be expressed in terms of the variation of the unit exergetic consumptions of each component: $\Delta\kappa_{ij} = \kappa_{ij}(\mathbf{x}) - \kappa_{ij}(\mathbf{x}_0)$, where κ_{ij} is the amount of exergetic resource that comes from the i-th component and it is necessary to obtain an exergy flow unit of the product of the j-th component, that is: $\kappa_{ij} = \dot{E}_{ij}/\dot{P}_j$.

After some algebraic manipulations of the variables of the PFR thermoeconomic model, the formula for the impact on fuel was obtained, as follow:

$$\Delta \dot{F}_T = \left(\Delta {}^t\boldsymbol{\kappa}_e + {}^t\boldsymbol{\kappa}_p^*(\mathbf{x})\Delta\langle \mathbf{KP}\rangle + {}^t\boldsymbol{\kappa}_p^*(\mathbf{x})\Delta\langle \mathbf{KR}\rangle\right)\mathbf{P}(\mathbf{x}_0) + {}^t\boldsymbol{\kappa}_p^*\Delta\mathbf{P}_s \quad (23)$$

The terms of equation can be understood as the contributions of:

$\Delta {}^t\boldsymbol{\kappa}_e\mathbf{P}(\mathbf{x}_0)$: variation in the unit exergy consumption of external resources, that is, of flows from the environment;

${}^t\boldsymbol{\kappa}_p^*(\mathbf{x})\Delta\langle \mathbf{KP}\rangle\mathbf{P}(\mathbf{x}_0)$: the variation in the unit exergy consumption of the component resources, whose exergy cost can be determined by the unit exergy costs of the resources used to compensate for the change in the operating condition;

${}^t\boldsymbol{\kappa}_p^*(\mathbf{x})\Delta\langle \mathbf{KR}\rangle\mathbf{P}(\mathbf{x}_0)$: the variation in the unit exergy consumption of the residue, because of the change in the operating condition of the system, which also causes a change in the unit exergy cost of the residue;

${}^t\boldsymbol{\kappa}_p^*\Delta\mathbf{P}_s$: the variation in the total product of the system caused by the adjustment of the operation of the components before the change in the operating condition of the system.

The 1% decrease in the isentropic efficiency of the compressor caused the gas turbine to consume an additional 4.05 MW of fuel to produce the same power (235 MW), as shown in Figure 7. The figure indicates the decomposition of consumption additional resources according to the expression of technical savings ($\Delta\dot{F}_T = \Delta\dot{I}_T + \Delta\dot{R}_T$). This decomposition revealed that the malfunction induced the generation of an additional 2.08 MW of residue, owing to the increase in the mass flows of the combustion gases at the exit of both chambers, because it was assumed that they exit at the same pressure and temperature in the absence and presence of a malfunction. This increase in residue generation was 51.30%, while the increase in the flow of irreversibility of the system components was 48.70% (1.97 MW).

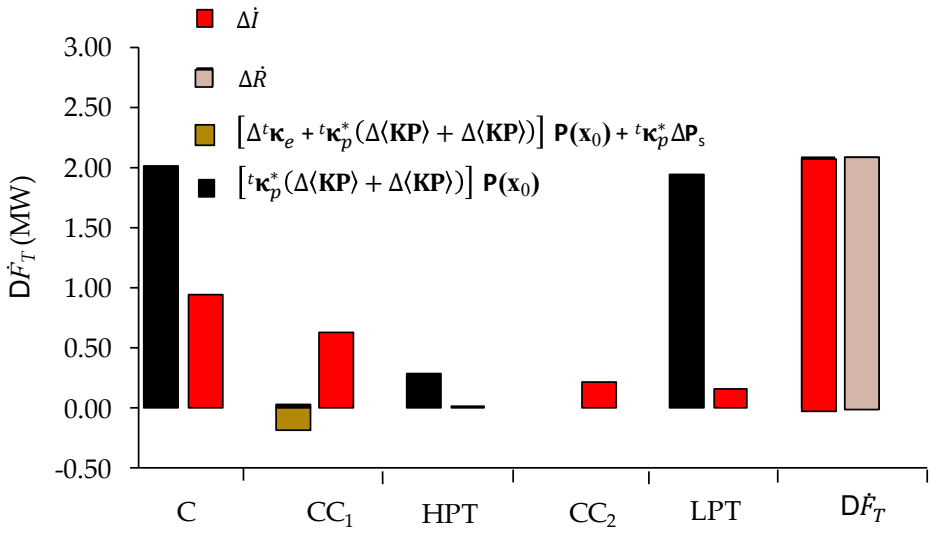


Figure 7. Impact on fuel and technical savings; compressor (C), first annular combustion chamber (CC_1), second annular combustion chamber (CC_2), high-pressure turbine (HPT), low-pressure turbine (LPT).

By decomposing the additional resource consumption using the fuel impact formula given by Equation (23) [20], we could identify that the compressor and the low-pressure turbine presented the highest increases in unit exergy costs, owing to the presence of the anomaly, which was captured using the following equation: $[{}^t\boldsymbol{\kappa}_p^*\,(\Delta\langle \mathbf{KP}\rangle + \Delta\langle \mathbf{KP}\rangle)]\mathbf{P}(\mathbf{x}_0)$. The cost of the malfunction in the compressor represented 49.52%, while that of the LPT represented 47.68%, of the total impact on the fuel (4.05 MW).

5.2. Malfunction and Dysfunction Analysis

It is well known that the more advanced a production process is, the higher the cost of irreversibilities and, therefore, the greater its impact on fuel consumption. The degradation of one component forces the others to adapt their performance to the new operating condition to maintain the same production and modify their irreversibility.

A 1% degradation of the compressor makes the components of the regenerative gas turbine to adapt their operation to supply the same electric power, and Figure 8 pretends illustrate this phenomenon. This figure also shows that C and CC are the equipment with the greatest contribution to the total increment of the system irreversibility, 0.95 MW and 0.65 MW, respectively (see Table 9).

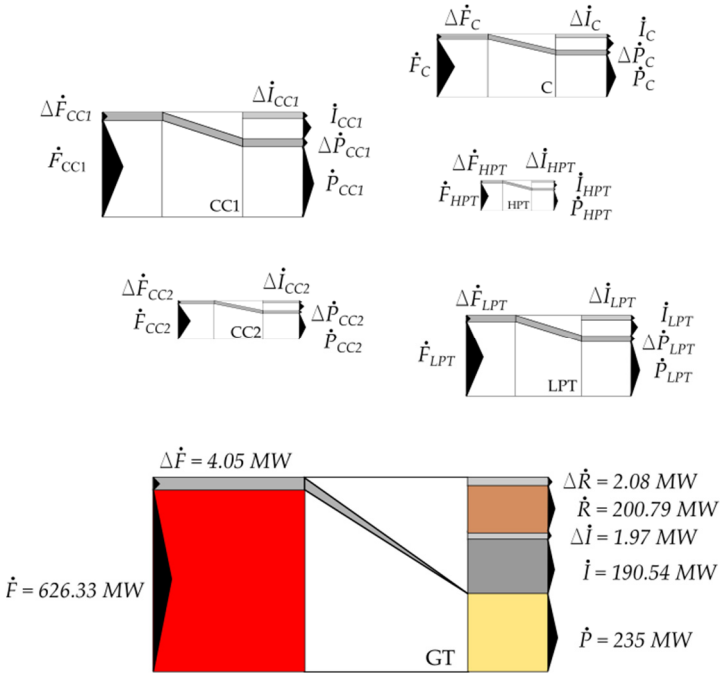


Figure 8. Impact on fuel consumption and generation of irreversibilities of a regenerative gas turbine that produces 235 MW corresponding to compressor degradation of 1%; compressor (C), first annular combustion chamber (CC_1), second annular combustion chamber (CC_2), high-pressure turbine (HPT), low-pressure turbine (LPT).

The presence of an anomaly in an energy system is accompanied by a variation in the consumption of resources if the system maintains the same production results; this can be expressed as follows:

$$\Delta\dot{F}_T = \Delta\dot{I}_T + \Delta\dot{R}_T \tag{24}$$

The impact on fuel consumption occurs to compensate for variations in the internal ($\Delta\dot{I}_T = \Delta\mathbf{I}\cdot\mathbf{u}$) and external ($\Delta\dot{R}_T = \Delta\mathbf{R}\cdot\mathbf{u}$) irreversibilities suffered by the system, to deal with the anomaly. The analysis of malfunctions and dysfunctions proposed by Valero et al. [19] was based on the decomposition of the variations of the internal ($\Delta\dot{\boldsymbol{I}}$) and external ($\Delta\dot{\boldsymbol{R}}$) irreversibilities of the components of the productive system, in terms of the unit consumption of resources and residuals, as shown in the following equations:

$$\Delta\dot{\mathbf{I}} = \Delta\mathbf{K}_\mathrm{D}\mathbf{P}(\mathbf{x}_0) + (\mathbf{K}_\mathrm{D} - \mathbf{U}_\mathrm{D})\Delta\mathbf{P} \tag{25}$$

$$\Delta\dot{\mathbf{R}} = \Delta\langle\mathbf{KR}\rangle\mathbf{P}(\mathbf{x}_0) + \langle\mathbf{KR}\rangle\Delta\mathbf{P} \tag{26}$$

From Equations (25) and (26), the variations in the irreversibilities can be expressed as $\Delta\dot{\boldsymbol{I}} + \Delta\dot{\boldsymbol{R}} = \mathbf{MF}_e^t + \mathbf{MF}^t + \mathbf{MR}^t + \mathbf{DF}$, in terms of malfunctions that are changes of the

endogenous irreversibilities that can be internal ($\mathbf{MF}_e^t + \mathbf{MF}^t$) or external ($\mathbf{MR}^t$), as well as dysfunctions (**DF**) that represent variations in the exogenous irreversibilities. The internal malfunction of a component is generated by the variation of the irreversibility in the component, due to the variation in its unit exergy consumption of resources from the environment, $\mathbf{MF}_e^t = (\Delta\mathbf{K}_\mathrm{D} - \Delta\mathbf{KP})\mathbf{P}(\mathbf{x}_0)$, or other productive components of the energy system, $\mathbf{MF}^t = \mathrm{D}\langle\mathbf{KP}\rangle\mathbf{P}(\mathbf{x}_0)$. The external malfunction is due to the production of residue variations in each component and can be expressed as: $\mathbf{MR}^\mathrm{t} = \mathrm{D}\langle\mathbf{KR}\rangle\mathbf{P}(\mathbf{x})$. The dysfunctions, $\mathbf{DF} = \left[\left|\dot{\mathbf{I}}\right\rangle(x) + \left|\dot{\mathbf{R}}\right\rangle(x)\right]\left(\mathbf{MF}^t + \mathbf{MR}^t\right)$ are variations associated with exogenous irreversibilities in a component and are induced by the malfunction of other components, which forces the component to consume more or less resources to satisfy its local production. The dysfunction of a component depends on its position in the system and can only be reduced if the anomaly is addressed. In this way, the impact on fuel consumption as a function of component malfunctions and dysfunctions can be expressed as follows:

$$\Delta\dot{F}_T = \mathbf{u}^t\left(\Delta\dot{\mathbf{I}} + \Delta\dot{\mathbf{R}}\right) = \mathbf{u}^t\left(\mathbf{MF}_e^t + \mathbf{MF}^t + \mathbf{MR}^t + \mathbf{DF}\right) \tag{27}$$

In thermoeconomic theory, internal and external malfunctions have an associated exergetic cost that corresponds to the sum of the malfunction of the component and the malfunctions and dysfunctions induced in the other components.

$$\mathbf{MF}_e^{*t} = \mathbf{MF}_e^t \tag{28}$$

$$\mathbf{MF}^{*t} = \mathbf{MF}^t + \left|\dot{\mathbf{I}}\right\rangle(x)\left(\mathbf{MF}^t + \mathbf{MR}^t\right) \tag{1}$$

$$\mathbf{MR}^{*t} = \mathbf{MR}^t + \left|\dot{\mathbf{R}}\right\rangle(x)\left(\mathbf{MF}^t + \mathbf{MR}^t\right) \tag{2}$$

At the beginning of Equation (27), it turns out that the impact on fuel can also be expressed as the sum of the cost of internal malfunctions $\left(\mathbf{MF}_e^{*t} + \mathbf{MF}^{*t}\right)$ and external ($\mathbf{MR}^{*t}$) according to the following expression:

$$\Delta\dot{F}_T = \mathbf{u}^t\left(\mathbf{MF}_e^{*t} + \mathbf{MF}^{*t} + \mathbf{MR}^{*t}\right) \tag{31}$$

The cost of each malfunction represents the additional fuel consumption of the system, owing to the existence of an intrinsic malfunction, such as the inefficiency of the corresponding component that forces the other components of the system to adapt their operating conditions and induce malfunctions.

Table 10 presents the decompositions of the impact on the fuel caused by the degradation of 1% in the compressor, in terms of the variations in the internal and external irreversibilities, malfunctions, and their costs, according to Equations (24), (27) and (31), respectively. The first two columns of this table indicate that the largest contributions to the impact on fuel corresponded to increases in the irreversibilities (23.46%, 0.95 MW) and residual (26.44%, 1.07 MW) in the compressor, which was expected given that failure occurred in this component. The degradation of the compressor increased the irreversibilities of the other equipment of the gas turbine with post-combustion and the residue attributed to the components involved in the residue formation, that is, in the compressor (1.07 MW) and in both combustion chambers (0.64 MW and 0.37 MW).

The next four columns (from 3 to 6) of Table 10 correspond to the decomposition of the impact on fuel in terms of malfunctions ($\mathbf{MF}_e^t$, $\mathbf{MF}^t$ y $\mathbf{MR}^t$) and dysfunctions (**DF**), according to Equation (32). Compressor degradation causes this component to have the highest contribution to fuel impact (49.90%, 2.02 MW) compared to the other components. This component presents the highest internal malfunction (MF_C = 1.15 MW), and a dysfunction of DF_C = 1.27 MW is induced.

Table 10. Impact decomposition on fuel.

	DI	DR	$\mathbf{MF_e^t}$	$\mathbf{MF^t}$	$\mathbf{MR^t}$	$\mathbf{DF_k}$	$\mathbf{MF_e^{*t}}$+MFR*$^{\mathbf{t}}$
				(MW)			
C	0.95	1.07	−0.40	1.15	0	1.27	2.02
CC1	0.64	0.64	0.94	−1.15	0.02	1.47	1.27
HPT	0.01	0	−0.10	0.10	0	0.01	0.01
CC2	0.21	0.37	0	0	0	0.59	0.59
LPT	0.16	0	−0.65	0.65	0	0.16	0.16
	1.97	2.08	−0.21	0.75	0.02	3.49	4.05

Combustion chamber 1 contributes second to the impact on fuel (31.94 %, 1.27 MW). To compensate for compressor degradation and for the gas turbine to generate the same power, CC_1 requires the highest consumption of external resources ($MF_{e,CC1}$ = 0.94 MW), and the greatest dysfunction is induced (DF_{CC1} = 1.47 MW).

The HPT, CC_2, and low-pressure turbine have zero malfunction values ($MF_{e,i}$ + MF_i + MR_i = 0, i = HPT, CC_2, and LPT); however, the malfunction of the remaining components of the gas turbine induced malfunctions in these equipment (DF_{HPT} = 0.01 MW, DF_{CC2} = 0.59 MW y DF_{LPT} = 0.16 MW).

The last column of Table 10 presents the sum of the costs of internal $\left(\mathbf{MF}_e^{*t} + \mathbf{MF}^{*t}\right)$ and external ($\mathbf{MR}^{*t}$) malfunctions of afterburner gas turbine components. The compressor presented the highest cost of malfunctions (2.02 MW), followed by combustion chamber 1 (1.27 MW), which was consistent with the fact that the compressor exhibits a degradation of 1% in its efficiency, and that the combustion chamber demands more fuel to sustain production.

6. Conclusions

This article is an application of thermoeconomic theory to an Alstom GT24 afterburner gas turbine. The study includes the study of the costs of formation of the functional product and the residues, which, from the construction of the productive structure of the gas turbine, were attributed to the productive components involved in its formation. The residues of the system were the residual heat (physical exergy) of the exhaust gases formed by the compressor and both combustion chambers, and the chemical exergy of the combustion gases formed in both combustion chambers. Likewise, through the application of the thermo-economic diagnosis, the importance of estimating the costs of the internal currents of the system is shown in the evaluation of the impact of the additional fuel requirements to compensate for possible malfunctions.

The case study corresponded to the Alstom GT24 afterburner gas turbine that generates an electrical power of 235 MW. Under design conditions, the exergetic efficiency of the gas turbine was 37.52% with a fuel requirement of 12.56 kg_{fuel}/s (10.16 kg_{fuel}/s for the first combustion chamber and 2.40 kg_{fuel}/s for the second one) and an air flow of 440.16 kg_a/s. The exergy cost of the power generated by the gas turbine was 626.33 MW, of which 30.42%, 29.22%, and 2.84% corresponded to the costs of irreversibility and the formation of physical and chemical residues, respectively. The first combustion chamber has the greatest contribution in the formation of physical residue; while the second one has the major responsibility in the formation of the chemical residue. The exergoeconomic cost of the electrical energy generated by the gas turbine was 10,098.71 USD/h and the thermoeconomic cost indicated that 34.76% and 65.24% represented the contributions associated with external resources, and capital and operating costs, respectively.

The 1% deterioration in the isentropic efficiency of the compressor makes the gas turbine require an additional 4.05 MW of fuel, causing increases of 1.97 MW and 2.08 MW in the generation of irreversibility and residue, respectively. Likewise, the additional fuel requirement in terms of internal and external malfunctions and malfunctions represents 0.54 MW, 0.02 MW and 3.49 MW, respectively. The compressor was the equipment that

generated the highest cost, which represented 49.9% of the additional requirement of the gas turbine. With the application of this methodology, it was possible to identify the origin of the anomaly, and to understand its impact in the operation of the rest of the components. The results of the work provide useful guidelines for subsequent study of symbolic thermoeconomics under design and off-design conditions.

Author Contributions: Conceptualization, H.L.-M., E.V.T.-G. and R.L.-L.; data curation, T.L.-A.; formal analysis, S.C.-H. and H.L.-M.; investigation, S.C.-H.; methodology, S.C.-H., E.V.T.-G., H.L.-M., T.L.-A. and R.L.-L.; project administration, R.L.-L.; software, S.C.-H. and H.L.-M.; supervision, H.L.-M. T.L.-A. and R.L.-L.; validation, H.L.-M., E.V.T.-G. and S.C.-H.; visualization, R.L.-L.; writing, original draft, S.C.-H.; writing, review and editing, H.L.-M., T.L.-A. and R.L.-L. All authors have read and agreed to the published version of the manuscript.

Funding: This research received no external funding.

Data Availability Statement: Not applicable.

Acknowledgments: S. Castro-Hernández gratefully acknowledges the scholarship from the Mexican National Council for Science and Technology (CONACyT) to pursue his postgraduate studies in UAM-Iztapalapa.

Conflicts of Interest: The authors declare no conflict of interest.

References

1. Heravi, G.; Salehi, M.M.; Rostami, M. Identifying Cost-Optimal Options for a Typical Residential Nearly Zero Energy Building's Design in Developing Countries. *Clean Technol. Environ. Policy* **2020**, *22*, 2107–2128. [CrossRef]
2. Ahmadi, P.; Dincer, I. Thermodynamic and Exergoenvironmental Analysis, and Multi-Objective Optimization of a Gas Turbine Power Plant. *Appl. Therm. Eng.* **2011**, *31*, 2529–2540. [CrossRef]
3. Ahmadi, P.; Dincer, I. Thermodynamic Analysis and Thermoeconomic Optimization of a Dual Pressure Combined Cycle Power Plant with a Supplementary Firing Unit. *Energy Convers. Manag.* **2011**, *52*, 2296–2308. [CrossRef]
4. Nadir, M.; Ghenaiet, A. Thermodynamic Optimization of Several (Heat Recovery Steam Generator) HRSG Configurations for a Range of Exhaust Gas Temperatures. *Energy* **2015**, *86*, 685–695. [CrossRef]
5. Frangopoulos, C.A. (Ed.) *Exergy, Energy System Analysis and Optimization-Volume II: Thermoeconomic Analysis Modeling, Simulation and Optimization in Energy Systems*; EOLSS Publications: Rio de Janeiro, Brazil, 2009; Volume 2.
6. Ahmadi, P.; Dincer, I. Exergoeconomics. In *Comprehensive Energy Systems*; Elsevier Inc.: Amsterdam, The Netherlands, 2018; Volume 1–5.
7. Casarosa, C.; Donatini, F.; Franco, A. Thermoeconomic Optimization of Heat Recovery Steam Generators Operating Parameters for Combined Plants. *Energy* **2004**, *29*, 389–414. [CrossRef]
8. Picallo-Perez, A.; Catrini, P.; Piacentino, A.; Sala, J.M. A Novel Thermoeconomic Analysis under Dynamic Operating Conditions for Space Heating and Cooling Systems. *Energy* **2019**, *180*, 819–837. [CrossRef]
9. Villalón, J.; Torrent, J.; Aragón, E. *Termoeconomía y Optimización Energética*; Fundación Gómez Pardo: Madrid, Spain, 2009.
10. Erlach, B. *Comparison of Thermoeconomic Methodologies: Structural Theory, AVCO and LIFO. Application to a Combined Cycle*; Department of Mechanical Engineering, University of Zaragoza: Zaragoza, Spain, 1998.
11. Lazzaretto, A.; Tsatsaronis, G. SPECO: A Systematic and General Methodology for Calculating Efficiencies and Costs in Thermal Systems. *Energy* **2006**, *31*, 1257–1289. [CrossRef]
12. Torres, C. *Termo-Economía. Curso de Doctorado*; Department of Mechanical Engineering, University of Zaragoza: Zaragoza, Spain, 1998.
13. Torres, C.; Valero, A.; Rangel, V.; Zaleta, A. On the Cost Formation Process of the Residues. *Energy* **2008**, *33*, 144–152. [CrossRef]
14. Agudelo, A.; Valero, A.; Torres, C. Allocation of Waste Cost in Thermoeconomic Analysis. *Energy* **2012**, *45*, 634–643. [CrossRef]
15. Lior, N. Sustainable energy development: A brief introduction to the present situation. In Proceedings of the 24th International Conference on Efficiency, Cost, Optimization, Simulation and Environmental Impact of Energy Systems, ECOS 2011, Novi Sad, Serbia, 4–7 July 2011.
16. Denise, L.H.; Vicente, T.E.; Sergio, C.; Martín, S.; Teresa, L.; Raúl, L. An Irreversibility-Based Criterion to Determine the Cost Formation of Residues in a Three-Pressure-Level Combined Cycle. *Entropy* **2020**, *22*, 299. [CrossRef] [PubMed]
17. Lozano, M.A.; Valero, A. *Thermoeconomic Analysis of a Gas Turbine Cogeneration System*; ASME Book No. H00874; ASME: New York, NY, USA, 1993; Volume 30, pp. 312–320.
18. Seyyedi, S.M.; Ajam, H.; Farahat, S. A New Criterion for the Allocation of Residues Cost in Exergoeconomic Analysis of Energy Systems. *Energy* **2010**, *35*, 3474–3482. [CrossRef]
19. Helen, L.M.; Sergio, C.H.; Martín, S.P.; Javier, V.L.; Vicente, T.G.E.; Raúl, L.L. Residue Cost Formation of a High Bypass Turbofan Engine. *Appl. Sci.* **2020**, *10*, 9060.

20. Torres, C.; Valero, A. The Exergy Cost Theory Revisited. *Energies* **2021**, *14*, 1594. [CrossRef]
21. Lozano, M.A.; Valero, A. Theory of the Exergetic Cost. *Energy* **1993**, *18*, 939–960. [CrossRef]
22. Torres, C.; Valero, A.; Serra, L.; Royo, J. Structural Theory and Thermoeconomic Diagnosis: Part I. *Energy Convers. Manag.* **2002**, *43*, 1503–1518. [CrossRef]
23. Sala, L.; Picallo, A. Operational Diagnosis of Thermal Installations in Buildings. In *Exergy Analysis and Thermoeconomics of Buildings*; Butterworth-Heinemann: Oxford, UK, 2020; pp. 721–788.
24. Valero, A.; Correas, L.; Zaleta, A.; Lazzaretto, A.; Verda, V.; Reini, M.; Rangel, V. On the Thermoeconomic Approach to the Diagnosis of Energy System Malfunctions: Part 2. Malfunction Definitions and Assessment. *Energy* **2004**, *29*, 1889–1907. [CrossRef]
25. Carapellucci, R.; Giordano, L. A Comparison between Exergetic and Economic Criteria for Optimizing the Heat Recovery Steam Generators of Gas-Steam Power Plants. *Energy* **2013**, *58*, 458–472. [CrossRef]
26. Perpignan, A.A.; Talboom, M.G.; Levy, Y.; Rao, A.G. Emission modeling of an interturbine burner based on flameless combustion. *Energy Fuels* **2018**, *32*, 822–838. [CrossRef] [PubMed]
27. Sabia, P.; Sorrentino, G.; Ariemma, G.B.; Manna, M.V.; Ragucci, R.; de Joannon, M. MILD combustion and biofuels: A minireview. *Energy Fuels* **2021**, *35*, 19901–19919. [CrossRef]